A Turnstile Junction Waveguide Orthomode Transducer for the 1 mm Band

Alessandro Navarrini, Richard L. Plambeck, and Daning Chow

***Abstract*—We describe the design and construction of a waveguide orthomode transducer (OMT) for the 200-270 GHz frequency band. The OMT provides a circular waveguide input (diameter 1.12 mm) and two WR3.7 rectangular waveguide outputs. It utilizes a turnstile junction and two E-plane power combiners. A tuning stub located at the base of the circular waveguide matches the input over the full frequency band.**

We have machined two such OMTs, but their performance has not yet been measured. Electromagnetic simulations predict a reflection coefficient at the circular input port below -20 dB for both polarizations and a transmission loss of ~0.6 dB at room temperature. When cooled to 4 K, the transmission loss is expected to be ~0.2 dB. In previous tests of a K-band scale model of the OMT, the measured performance matched the theoretical results closely.

***Index Terms*— Radio astronomy, Turnstile junction, Power combiner, Polarimetry, Waveguide transitions**

I. Introduction

We are constructing orthomode transducers for dual polarization 200-270 GHz radio astronomy receivers on the CARMA array. In order to fit into the existing dewars, the OMTs must be compact; hence we strongly prefer to use waveguide-based designs rather than wire grid polarizers.

Wollack amd Grammer [1] constructed a waveguide OMT based on a Bøifot junction that gave excellent performance over the 211-275 GHz band. We felt that this OMT would be challenging for us to mass produce because it requires careful alignment of a 0.036 mm thick septum and four 0.061 mm diameter capacitive compensation pins inside the waveguides. Other designs using a thicker septum have been proposed; here the pins are eliminated in favor of short capacitive steps [2] or standard multi-step transitions on the side arms [3]. Although in these cases the construction of the blocks is simplified, the alignment of the septum inside the waveguide is still critical.

In [4] we described an alternative to the Bøifot OMT that is based on a turnstile junction. An advantage of this design is that neither the pins nor the septum of the Bøifot junction are required to achieve polarization separation and low VSWR over a wide bandwidth; in addition, all rectangular waveguides can be split along their midplanes. As reported in [4], we constructed and tested a K-band version of the turnstile OMT. From 18-26 GHz we measured an input reflection coefficient of less than -16 dB, a cross-polarization of less than -47 dB, and a transmission loss of ~0.1 dB. We also used electromagnetic simulations to estimate the degradation in performance that machining errors of ± 0.13 mm would cause in the 18-26 GHz band, with the expectation that the fabrication tolerances could be held to ± 13 μm for a 200-270 GHz OMT.

Here we describe the design and construction of a 1mm version of the turnstile OMT. Two have been machined so far, but have not yet been tested.

The authors are with the Radio Astronomy Laboratory, University of California, Berkeley, CA 94720 (e-mail: navarrin@astro.berkeley.edu).

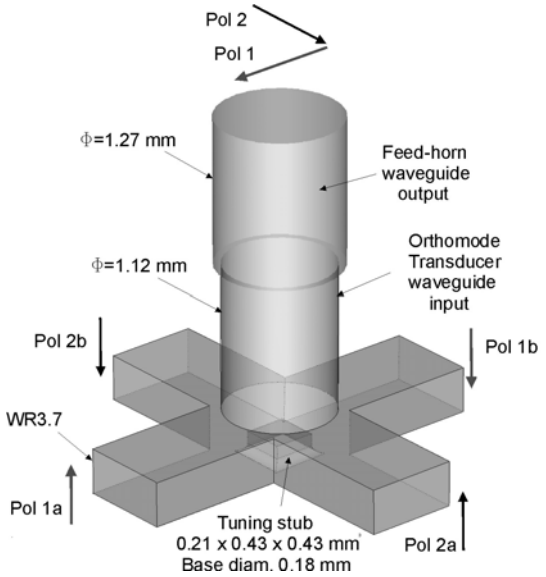

Fig. 1. Internal view of the turnstile junction with a circular waveguide input and four full-height waveguide outputs. The tuning stub is optimized for broadband performance. The circular waveguide on top represents the output of the 1 mm feed horn to which the OMT will attach.

II. Design and Optimization

As shown in Fig. 1, the turnstile junction uses a round input waveguide and four rectangular output waveguides. We note that a Bøifot junction is essentially a turnstile in which two of the arms have been folded around a septum. After emerging from the turnstile, signals in opposite pairs of waveguides are combined in power combiners before they are directed to two output waveguides.

The input circular waveguide on the turnstile junction has a diameter D = 1.12 mm, but attaches to the D = 1.27 mm circular waveguide at the output of the existing feed horns. The reflection coefficient caused by this step in the waveguide diameter is below –30 dB over most of the band. The

rectangular waveguides are full height WR3.7 (0.94 mm x 0.47 mm).

In addition to the fundamental TE_{11} modes associated with the orthogonal polarizations, the circular waveguide can propagate higher-order modes in the 200-270 GHz frequency band. These are the TM_{01} mode, with λ_c~1.306 D (ν_c=205.0 GHz), and the TE_{21} mode with λ_c~1.028 D (ν_c=260.5 GHz). In theory, these modes can be excited by the discontinuity created by the sidearm junctions. However, their excitation can be avoided as long as the four-fold symmetry of the structure is maintained.

The metallic tuning stub located at the base of the circular waveguide enables broadband operation with low reflection coefficient. The stub is a square prism with dimensions 0.43 mm x 0.43 mm x 0.21 mm, centered on the circular waveguide axis. The base is filleted with radius 0.09 mm so the stub can be machined from the side. The structure was optimized using the electromagnetic simulator CST Microwave Studio [5] based on the finite integration technique. Fig. 2 shows the simulation result for the reflected amplitude of the TE_{11} mode at the 1.27 mm diameter circular waveguide input, with all four rectangular ports terminated with matched loads. The reflection coefficient is below -28 dB over the frequency range of interest.

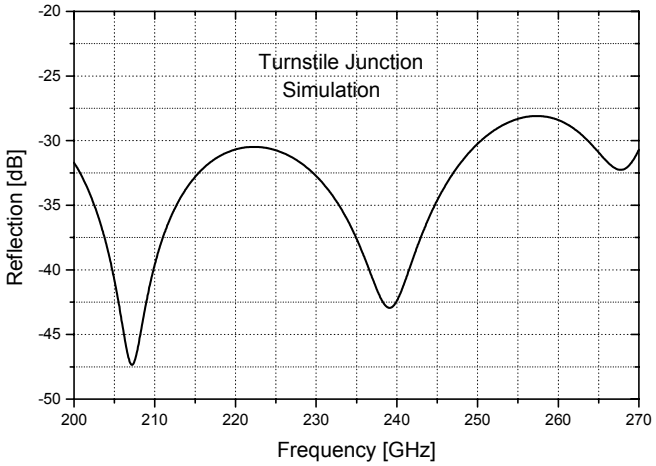

Fig. 2. Simulated reflected amplitude for a TE_{11} mode at the circular waveguide port of the five-port device illustrated in Fig. 1.

Figure 3 shows the complete OMT. Signals split by the turnstile junction exit opposite waveguides 180^0 out of phase. These signals are recombined in a power combiner that also is 180^0 out of phase, implemented using the E-plane Y-junction shown in Fig. 4. The electrical lengths of the waveguides from the turnstile to the power combiner are kept equal to maintain the 180^0 phase shift. The combiner was based on a W-band design by Kerr [6] and was further optimized using CST Microwave Studio. The steps of the three-section transformer are filleted so they can be machined with an 0.45 mm diameter end-mill. The cusp at the junction of the curved arms is truncated at a width of 0.05 mm. Fig. 5 shows the simulated reflection coefficient at the WR3.7 common port when the two curved arms are terminated with matched loads. It is below –30 dB from 200-270 GHz.

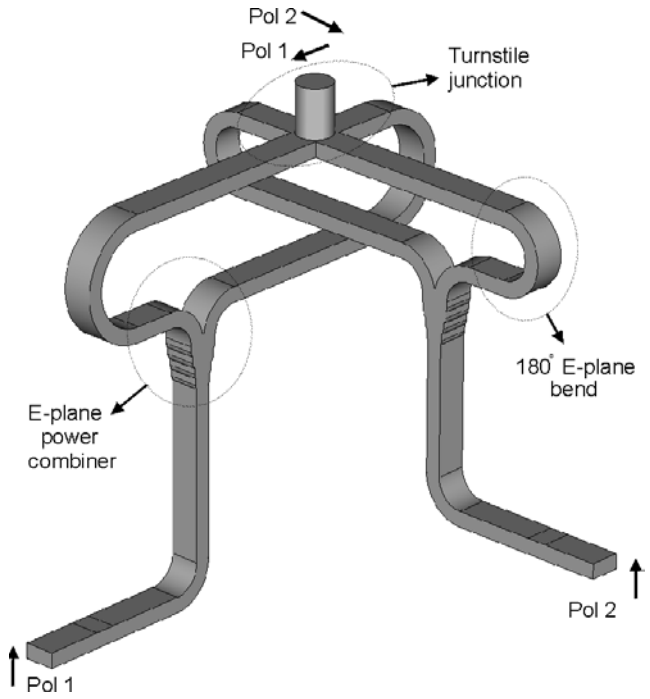

Fig. 3. Internal view of the full OMT. Opposite ports of the turnstile junction are brought together with E-plane bends and power combiners.

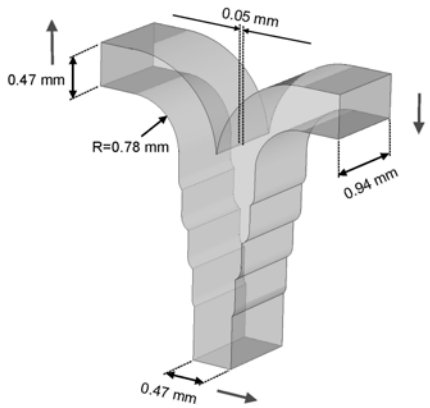

Fig. 4. Internal view of the E-plane Y-junction used to recombine the 180^0 out of phase signals at the output of the turnstile junction.

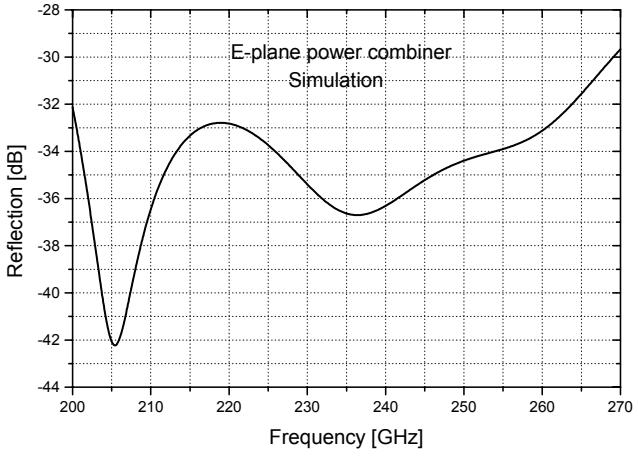

Fig. 5. Simulated reflection coefficient at the common waveguide port of the three-port device illustrated in Fig. 4.

The inside radius of the waveguide bends is 1.41 mm for Pol 1 and 0.78 mm for Pol 2. Electromagnetic simulation shows that even the tighter bend has reflection coefficient below –38 dB across the full waveguide band.

After recombination in the Y-junction, each signal is directed to its output flange through a 90^0 E-plane bend with inner radius 0.78 mm.

Figs. 6 and 7 show the simulated reflection coefficient and transmission losses for both polarization channels of the full OMT. The simulation was performed with the three-port model shown in Fig. 3, including the turnstile junction, power combiners, and all connecting waveguides. The model included the short section of 1.27 mm diameter circular waveguide at the input port to take into account the discontinuity at the feed-horn/OMT interface. A Cartesian mesh was automatically generated and the time domain solver calculated the broadband response of the device in one simulation run. We set the parameter "lines per wavelength" to 12; this is the minimum number of mesh lines per wavelength in each coordinate direction for the shortest wavelength in the simulation.

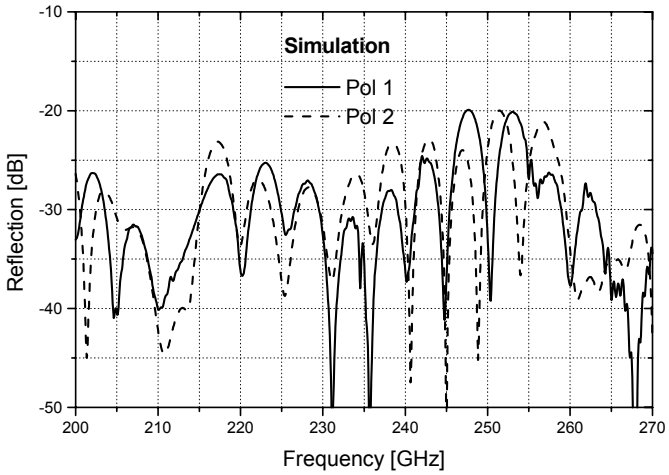

Fig. 6. Simulated Pol 1 (solid line) and Pol 2 (dotted line) amplitude reflection of TE_{11} mode at the circular waveguide output of the feed-horn when looking into the OMT input. The simulation refers to the 3-port device illustrated in Fig. 3 modified to include the abrupt transition between circular waveguides shown in Fig. 1.

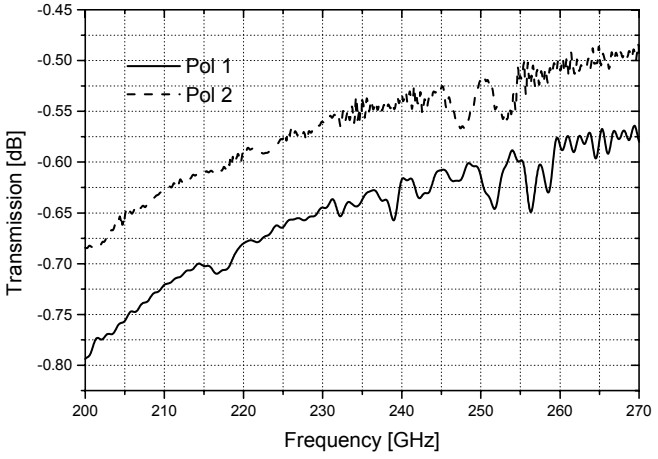

Fig. 7. Simulated room temperature transmission losses for Pol 1 (solid line) and Pol 2 (dotted line) of the OMT. We assumed a conductivity of half the dc value of gold $\sigma_{Au}=(4.26\cdot10^7)/2\ \Omega^{-1}m^{-1}$.

The predicted reflected amplitude at the circular waveguide port is below –20 dB for both polarizations between 200 GHz and 270 GHz. The room temperature transmission loss is below 0.8 dB for both polarizations. For this calculation we assumed the blocks are plated with pure gold and used a gold conductivity of half its dc value. For comparison, we estimate the theoretical room temperature loss [7] of a straight section of WR3.7 waveguide with perfectly smooth surfaces and a conductivity $\sigma_{Au}=(4.26\cdot10^7)/2\ \Omega^{-1}m^{-1}$ to be in the range 0.18-0.26 dB/cm between 200-270 GHz.

The electrical path length from the circular waveguide at the input of the OMT to the WR3.7 waveguide outputs is 30 mm for Pol 1 and 26 mm for Pol 2. The 0.1 dB higher insertion loss predicted for Pol 1 compared to Pol 2 is consistent with its 4 mm extra length.

The insertion loss of the OMT is expected to decrease by a factor of ~3 when it is cooled to cryogenic temperatures [8]. Therefore, we expect insertion losses in the range 0.16-0.27 dB when the OMT is operated at 4 K in front of SIS mixers.

III. Mechanical Design

The OMT is constructed by dividing the structure of Fig. 3 into four blocks that intersect along the circular waveguide axis. This allows all rectangular waveguides to be split along their midplanes. The power combiner for Pol 1 could be located along the central axis of the structure, but it is deliberately offset so that the sharp cusp of the Y-junction does not coincide with the plane where two blocks join. The tuning stub at the center of the turnstile junction is split into four identical sections that are machined at the same time as the rectangular waveguides.

The top of the OMT accepts a standard UG387 flange so it can mate with our existing feed horns. Although the locating pins for this flange are on the normal 14.29 mm diameter bolt circle, it was not possible to locate the waveguide screws in their normal positions, so a special clamp will be made to attach the flange. Custom mini-flanges, rather than standard UG387 flanges, are used for the output waveguides. Reducing the flange diameter allows the OMT to be smaller, hence reduces the waveguide lengths and insertion losses. The alignment pins and screw holes in the mini-flanges are on a 7.11 mm diameter bolt circle.

Thus far we have machined two OMTs on our numerically controlled milling machine. To minimize setup time, we machine all four blocks at one time as part of a single 12.7 x 12.7 x 165 mm metal bar. The bar is mounted to a tool steel fixture on the milling machine table with five 10-32 screws. A light cut is taken off one surface of the bar, then the fixture is rotated to expose the second surface of the bar and a light cut is taken off this surface as well. The waveguide circuitry, screw holes, and alignment pin holes are cut into this face of the four blocks in one pass, then the fixture is rotated back to the original position and the waveguide circuitry and holes are cut into the first face of the four blocks, again in one pass. Figure 8 shows the bar after it is removed from the fixture. To complete the OMT, the bar is cut into four sections; these are

aligned with 2.38 mm diameter dowel pins and bolted together. Finally, the outer surfaces are faced off and the round input waveguide and associated mounting holes are machined into the top face of the OMT.

Figs. 9-12 show photos of, respectively, one of the blocks in detail, all four unassembled blocks, the mated block pairs, and the fully assembled OMT. The final OMT, after finish of the surfaces, is a cube 23 mm on a side.

From the electromagnetic simulations described in [4] we estimate that machining tolerances must be ±10 μm to avoid degrading the OMT performance. Four types of mechanical imperfections were considered in these simulations: a difference in lengths of the opposite waveguide arms between the turnstile junction and the power combiner; a tuning stub that was too high; a circular waveguide offset from the intersection of the four blocks; and a difference in the height of the four quadrants of the tuning stub. Among the fabrication and alignment errors considered, differences in the lengths of the waveguide sidearms, between the turnstile junction and the power combiner, are the most harmful. These cause the appearance of a series of narrow resonances regularly spaced in frequency.

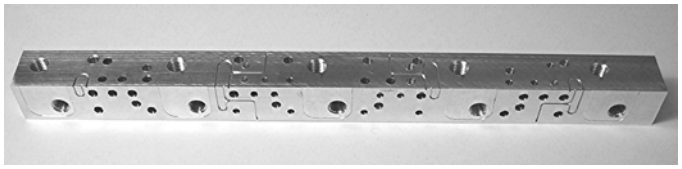

Fig. 8. View of the aluminum bar showing the machined waveguide circuitry of the two internal faces of the OMT. The bar is later cut in four parts which are assembled to form the OMT.

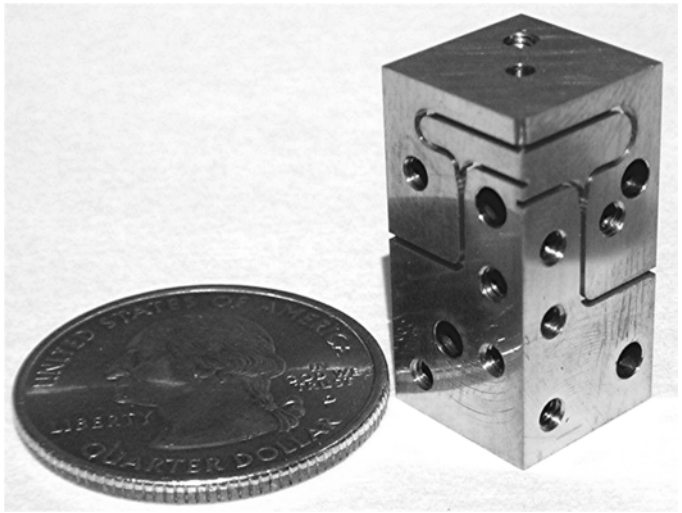

Fig. 9. View of one of the four TeCu blocks of the OMT showing the internal waveguide circuitry of turnstile junction, bends, and power combiners.

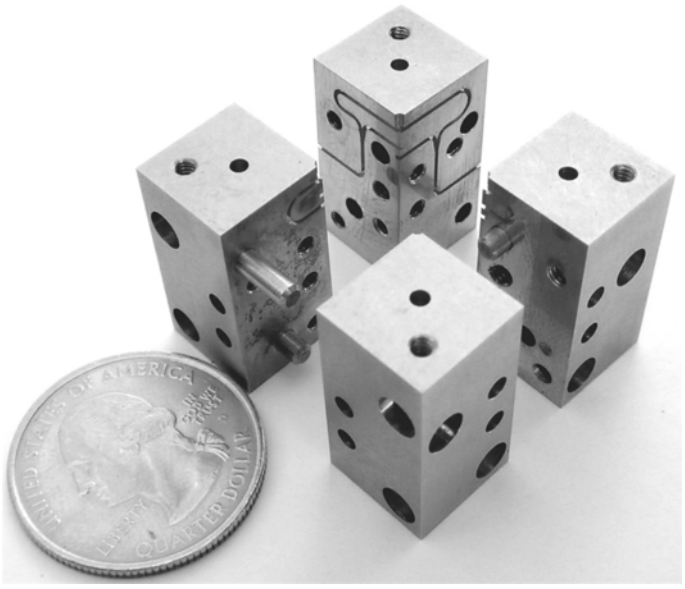

Fig. 10. View of the four blocks of the OMT.

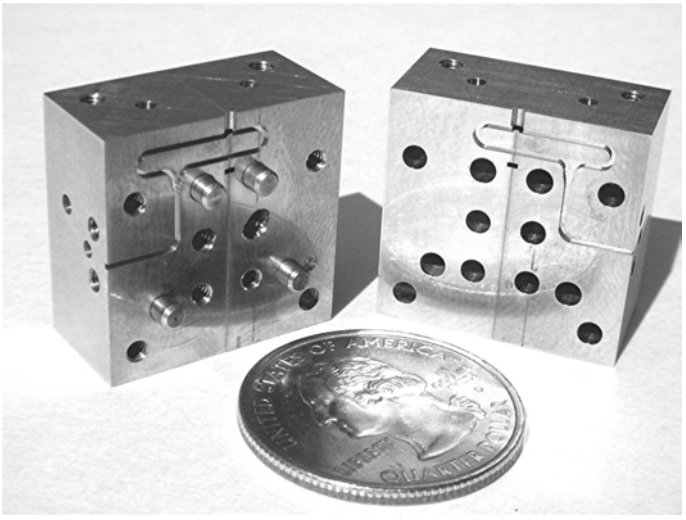

Fig. 11. View of assembled mating pairs of blocks showing the waveguide circuitry for Pol 2.

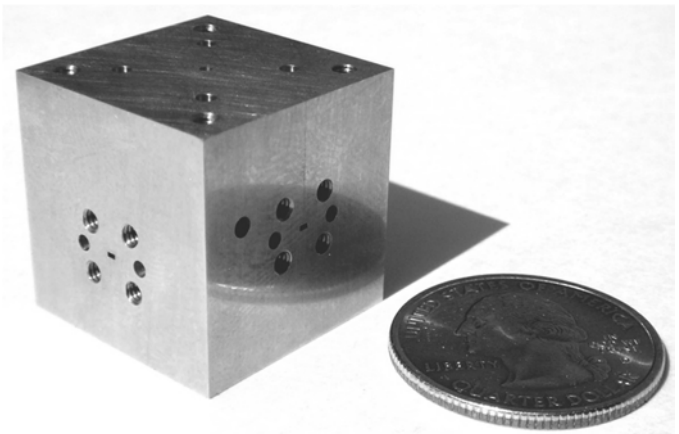

Fig. 12. View of assembled OMT with the circular waveguide input on top and the two WR3.7 waveguide outputs with custom mini-flanges. The external dimensions are 23 mm x 23 mm x 23 mm.

IV. Conclusion

We presented the design of an OMT with a circular waveguide input (diameter 1.12 mm) and two WR3.7 waveguide outputs for the 200-270 GHz band. The OMT utilizes a turnstile junction and two E-plane power combiners. A tuning stub located at the base of the circular waveguide matches the input over a broad frequency band.

The predicted amplitude of the reflection coefficient at the circular input port is below -20 dB for both polarization channels from 200-270 GHz.

The OMT is constructed from four blocks that intersect along the circular waveguide axis. Room temperature insertion losses below 0.8 dB are predicted. From simulation we estimate that machining tolerances must be within ±10 μm to avoid degraded performance.

References

[1] E. J. Wollack and W. Grammer, "Symmetric Waveguide Orthomode Junctions," *Proceedings of the 14th. International Symposium on Space Terahertz Technology*, Tucson, Arizona, Apr. 2003, pp 169-176.

[2] G. Narayanan and N. Erickson, "Full-Waveguide Band Orthomode Transducer for the 3 mm and 1mm Bands," *Proceedings of the 14th International Symposium on Space Terahertz Technology*, Tucson, Arizona, Apr. 2003, pp 508-512.

[3] A. Navarrini, and M. Carter, "Design of a Dual Polarization SIS Sideband Separating Receiver Based on Waveguide OMT for the 275-370 GHz Frequency Band," *Proceedings of the 14th International Symposium on Space Terahertz Technology*, Tucson, Arizona, Apr. 2003, pp 159-168.

[4] A. Navarrini and R. L. Plambeck, "A Turnstile Junction Waveguide Orthomode Transducer," *IEEE Trans. Microwave Theory Tech.* submitted.

[5] CST Microwave Studio. Büdinger Str. 2 a, D-64289 Darmstadt, Germany.

[6] A. R. Kerr, "Elements for E-plane Split-Blocks Waveguide Circuits," National Radio Astronomy Observatory, ALMA Memo No. 381, Jul. 2001.

[7] A. F. Harvey "Microwave Engineering," Academic Press Inc. London, 1963, pp. 15.

[8] E. J. Wollack, W. Grammer, J. Kingsley, "The Bøifot Orthomode Junction," ALMA Memo No. 425, May 2002.

A. Navarrini (S.M. '96-Ph.D '02) received an S. M. degree in physics from the University of Florence, Italy, in '96. After one year of graduate research in optoelectronics at University of College London he started to work on heterodyne instrumentation at IRAM, France, where he completed his Ph. D. in '02.

He is currently a postdoctoral fellow at the Radio Astronomy Lab at the University of California, Berkeley. His research interests include superconducting devices, low noise heterodyne instrumentation, submillimeter and quasioptical techniques, analysis of 3-D electromagnetic problems, and star formation.

R. L. Plambeck (S.B. '71-Ph.D '79) received an S.B. from M.I.T. and a Ph.D. from the University of California, both in Physics. Since 1979 he has worked at the University of California Radio Astronomy Lab, currently as Research Astronomer. His interests are in observational millimeter astronomy, particularly star formation, and in low-noise instrumentation.

D. Chow (S.B. '81) received an S.B. from College of South China. He is a Principle Laboratory Machinist for the Radio Astronomy Lab, University of California, Berkeley since 1990. He has worked extensively on precision machining of microwave and millimeter-wave components. His work includes manufacturing prototype mixer blocks, filters, feeds and orthomode transducers.